ELSEVIER

Fusion Engineering and Design 63–64 (2002) 569–575

Fusion Engineering and Design

www.elsevier.com/locate/fusengdes

Nonlinear Lyapunov-based burn control in fusion reactors

Eugenio Schuster *, Miroslav Krstić [1], George Tynan [2]

Department of Mechanical and Aerospace Engineering, University of California at San Diego, La Jolla, CA 92093-0411, USA

Abstract

Control of plasma density and temperature magnitudes, as well as their profiles, are among the most fundamental problems in fusion reactors. Existing efforts on model-based control use control techniques for linear models. In this work, a zero-dimensional (0-D) nonlinear model involving approximate conservation equations for the energy and the densities of the species was used to synthesize a nonlinear feedback controller for stabilizing the burn condition of a fusion reactor.

Keywords: Burn control; Fusion reactors; Nonlinear Lyapunov-based control

1. Introduction

In order to be commercially competitive, a fusion reactor needs to run long periods of time in a stable burning plasma mode at working points which are characterized by a high Q, where Q is the ratio of fusion power to auxillary power. Although operating points with these characteristics that are inherently stable exist for most confinement scalings, they are found in a region of high temperature and low density. Unfortunately, economical and technological constraints may require fusion reactors to operate in a zone where the thermonuclear reaction is inherently thermally unstable.

The common denominator of existing works is the approximation of the nonlinear model of the fusion reactor by a linearized one for the purpose of control design [1]. The nonlinear model is linearized, the controller is synthesized using linear control techniques and the performance of the resulting linear controller is tested through simulations that use the original nonlinear model. When tested through nonlinear simulations, these linear controllers succeed in stabilizing the system only against a limited set of perturbations in the initial conditions. In this work we present a stabilizing controller for the burn condition in fusion reactors synthesized using model-based nonlinear control techniques that avoid the linearization of the model. The avoidance of the linearization allows us to achieve much higher levels of performance and robustness.

Over the years, the physical and technological feasibility of different methods for controlling the burn condition have been studied [2–4]. In this

* Corresponding author. Tel.: +1-858-822-1936; fax: +1-858-822-3107

E-mail addresses: schuster@mae.ucsd.edu (E. Schuster), krstic@ucsd.edu (M. Krstić), gtynan@ucsd.edu (G. Tynan).

[1] Tel.: +1-858-822-1374.

[2] Tel.: +1-858-534-9724.

0920-3796/02/$ - see front matter
PII: S0920-3796(02)00272-7

work, we consider the use of auxiliary power and fueling rate modulations for stabilizing the burn condition of a fusion reactor working at a subignited point against a limited range of perturbations in the initial conditions. However, when we want to work at an ignited point or we want to have the capability of rejecting a larger set of perturbations in the initial conditions, we consider the controlled injection of impurities as an additional actuator.

The paper is organized as follows. In Section 2 the model of our plant is stated. In Section 3 the control objectives are presented and the stabilizing control laws for the different actuators are introduced in Section 4. Section 5 makes a presentation of the simulation results. The conclusions and some suggestions about future work are presented in Section 6.

2. Model

In this work, we use a zero-dimensional (0-D) model for a fusion reactor which employs approximate particle and energy balance equations. This is fundamentally the same model used by Hui, Fischbach, Bamieh and Miley [7] but we introduce a new equation for the dynamics of the injected impurities. The alpha-particle balance is given by

$$\frac{dn_\alpha}{dt} = -\frac{n_\alpha}{\tau_\alpha} + \left(\frac{n_{DT}}{2}\right)^2 \langle \sigma v \rangle \tag{1}$$

where n_α and n_{DT} are the alpha and deuterium–tritium (DT) densities, respectively, and τ_α is the confinement time for the alpha particles. A first order lag is introduced to take into account the diffusion time for neutral fuel atoms to transport into the Tokamak core. This lag runs from the start of the fuel injection to the change in DT ion particle density. The set of equations governing the neutral fuel atom balance and the DT ionized fuel particle balance is given by

$$\frac{dn_{DT}}{dt} = -\frac{n_{DT}}{\tau_{DT}} - 2\left(\frac{n_{DT}}{2}\right)^2 \langle \sigma v \rangle + \frac{n_n}{\tau_d} \tag{2}$$

$$\frac{dn_n}{dt} = -\frac{n_n}{\tau_d} + S \tag{3}$$

where n_n is the neutral fuel density, defined as the number of neutral fuel atoms divided by the core volume, S (input) is the refueling rate (50:50 D–T), defined as the number of neutral fuel atoms injected per unit time divided by the core volume, τ_{DT} is the confinement time for the ionized fuel particles and τ_d is the controller lag time. The impurity presence is determined by the balance equation

$$\frac{dn_I}{dt} = -\frac{n_I}{\tau_I} + S_I \tag{4}$$

where n_I is the impurity density, τ_I is the confinement time for the impurities and S_I (input) is the impurity injection rate. The energy balance is given by

$$\frac{dE}{dt} = -\frac{E}{\tau_E} + P_\alpha + P_{ohmic} - P_{rad} + P_{aux} \tag{5}$$

where E is the plasma energy, τ_E is the energy confinement time, $Q_\alpha = 3.52$ MeV is the energy of the alpha particles and P_{aux} (input) is the auxiliary power. $P_\alpha = (n_{DT}/2)^2 \langle \sigma v \rangle Q_\alpha$ is the alpha power and the ohmic power is written as $P_{ohmic} = \eta j^2$ where η is the Spitzer resistivity and j is the plasma current density. The radiation loss P_{rad} is given by

$$P_{rad} = [\psi_{DT}(T) n_{DT} + \psi_\alpha(T) n_\alpha + \psi_I(T) n_I] n_e \tag{6}$$

where the radiation due to the DT particles is bremsstrahlung radiation $\psi_{DT} = \psi_{brem} = A_b \sqrt{T}$ and the radiation losses due to the alpha and impurity particles are computed according to the law

$$\psi_Z(T) = 10^{\sum_{i=0}^{5} A_i^Z \{\log[T \text{ (keV)}]\}} \tag{7}$$

where Z is the type of ion and the constant parameters A_i can be found in [8]. The DT reactivity $\langle \sigma v \rangle$ is a highly nonlinear, positive and bounded function of the plasma temperature T given by

$$\langle \sigma v \rangle = \exp\left(\frac{a_1}{T^r} + a_2 + a_3 T + a_4 T^2 + a_5 T^3 + a_6 T^4\right)$$

and its parameters a_i and r taken from [9].

No explicit evolution equation is provided for the electron density n_e since we can obtain it from the neutrality condition $n_e = n_{DT} + 2n_\alpha + Z_I n_I$,

where Z_I is the atomic number of the impurities, whereas the total density and the energy are written as $n = 2n_{DT} + 3n_\alpha + (Z_I + 1)n_I$ and $E = 3nT/2$.

The energy confinement scaling used in this work is ITER90H-P [10] because it allows the comparison with previous linear controllers based on this scaling. However, it will be clear from the synthesis procedure that the results can be extended to newer scalings. This scales with plasma parameters as

$$\tau_E = f 0.082 I^{1.02} R^{1.6} B^{0.15} A_i^{0.5} \kappa_\chi^{-0.19} P^{-0.47} = kP^{-0.47}$$

where the isotopic number A_i is 2.5 for the 50:50 D–T mixture, the ITER machine parameters can be obtained from [11] and the factor scale f depends on the confinement mode. The isotopic number, factor scale and ITER machine parameters can be rewritten as a constant k because it is assumed that a magnetic controller is regulating these variables. The net plasma heating power is defined as $P = P_\alpha - P_{rad} + P_{aux} + P_{ohmic}$.

The net plasma heating power is compared with the L–H transition power (threshold power) P_{thr} to determine the value of f. This threshold power can be written as [12] $P_{thr} = 2.84 M^{-1} B^{0.82} n_e^{0.58} R^{1.00} \alpha^{0.81}$ where the units are amu, T, 10^{20} m^{-3} and m. When P drops below P_{thr} we adopt $f = f^L = f^H/2$, where $f^H = 0.85$. The confinement times for the different species are scaled with the energy confinement time τ_E as $\tau_\alpha = k_\alpha \tau_E$, $\tau_{DT} = k_{DT}\tau_E$ and $\tau_I = k_I \tau_E$. We also scale lag time with the energy confinement time as $\tau_d = k_d \tau_E$. For synthesis and simulation purposes we choose $k_d = 1$ arbitrarily which represents an appreciable lag in the actuation.

3. Control objective

The possible operating points of the reactor are given by the equilibria of the dynamic equations. The values of the variables at the equilibrium are denoted by a bar. An ignition point is characterized by $\bar{P}_{aux} = 0$ while at a subignition point we have $\bar{P}_{aux} > 0$. In this case we look for those operating points where $\bar{S}_I = 0$ because we are interested in an operating condition free of impurities. The density state variables $\bar{n}_\alpha$, $\bar{n}_{DT}$, $\bar{n}_\alpha$, $\bar{n}_I$ energy state variable $\bar{E}$ and inputs $\bar{P}_{aux}$, $\bar{S}$ at the equilibrium, are calculated as solutions of the nonlinear algebraic equations obtained by setting the left hand sides in equations Eqs. (1)–(5) to zero. Taking into account that $\bar{S}_I = 0$ and $\bar{n}_I = 0$, we define the deviations from the desired equilibrium values as $\tilde{n}_\alpha = n_\alpha - \bar{n}_\alpha$, $\tilde{n}_{DT} = n_{DT} - \bar{n}_{DT}$, $\tilde{n}_n = n_n - \bar{n}_n$, $\tilde{n}_I = n_I - \bar{n}_I = n_I > 0$, $\tilde{E} = E - \bar{E}$, $\tilde{P}_{aux} = P_{aux} - \bar{P}_{aux}$, $\tilde{S} = S - \bar{S}$ and $\tilde{S}_I = S_I - \bar{S}_I = S_I > 0$, we write the dynamic equations for the deviations as

$$\frac{d\tilde{n}_\alpha}{dt} = -\frac{\tilde{n}_\alpha}{\tau_\alpha} + \left[\left(\frac{\tilde{n}_{DT}}{2}\right)^2 + \frac{1}{2}\,\tilde{n}_{DT}\bar{n}_{DT}\right]\langle\sigma v\rangle + u_\alpha \tag{8}$$

$$\frac{d\tilde{n}_{DT}}{dt} = -\frac{\tilde{n}_{DT}}{\tau_{DT}} - \left[2\left(\frac{\tilde{n}_{DT}}{2}\right)^2 - \tilde{n}_{DT}\bar{n}_{DT}\right]\langle\sigma v\rangle + \frac{\tilde{n}_n}{\tau_d} + u_{DT} \tag{9}$$

$$\frac{d\tilde{n}_n}{dt} = S^* \tag{10}$$

$$\frac{d\tilde{n}_I}{dt} = -\frac{\tilde{n}_I}{\tau_I} + S_I \tag{11}$$

$$\frac{d\tilde{E}}{dt} = -\frac{\bar{E}}{\tau_E} - \left\{\frac{\bar{E}}{\tau_E} - [P_\alpha + P_{ohmic} - P_{rad} + P_{aux}]\right\} \tag{12}$$

where

$$u_\alpha = -\frac{\bar{n}_\alpha}{\tau_\alpha} + \left(\frac{\bar{n}_{DT}}{2}\right)^2\langle\sigma v\rangle \tag{13}$$

$$u_{DT} = -\frac{\bar{n}_{DT}}{\tau_{DT}} - 2\left(\frac{\bar{n}_{DT}}{2}\right)^2\langle\sigma v\rangle + \frac{\bar{n}_n}{\tau_d} \tag{14}$$

$$S^* = -\frac{\tilde{n}_n}{\tau_d} + \tilde{S} - \frac{\bar{n}_n}{\tau_d} + \bar{S} = -\frac{n_n}{\tau_d} + S \tag{15}$$

The control objective is to drive the initial perturbations in $\tilde{n}_\alpha$, $\tilde{n}_{DT}$, $\tilde{n}_n$, $\tilde{n}_I$, $\tilde{E}$ to zero using actuation through P_{aux}, S and $S_I = \tilde{S}_I > 0$. It is important to note that in the ignition case ($\bar{P}_{aux} = 0$) we have $\tilde{P}_{aux} > 0$ as a constraint, we do not have the possibility of modulating P_{aux} in both the positive and negative sense. However, the additional actuator $S_I = \tilde{S}_I > 0$, although constrained

in sign by itself, will help us to overcome the constraint in P_{aux}. All the states are assumed to be available for feedback, either by measurement or by estimation.

4. Controller design

We start by looking for a control, which stabilizes $\tilde{E}$. We choose P_{aux} and $P_{rad}(n_I)$ in order to reduce Eq. (12) to

$$\frac{d\tilde{E}}{dt} = -K_E \frac{\tilde{E}}{\tau_E}, \quad K_E > 0$$

This means we choose P_{aux} and $P_{rad}(n_I)$ such that

$$-K_E \frac{\tilde{E}}{\tau_E} = -\frac{\tilde{E}}{\tau_E} - \frac{\bar{E}}{\tau_E} + P_\alpha + P_{ohmic} - P_{rad} + P_{aux} \tag{16}$$

The gain K_E allows us to regulate the response rate of $\tilde{E}$. This helps us to regulate the control force in order to keep the modulation rate of the auxiliary power in MW s^{-1} below the technological limits. Nevertheless the computation of P_{aux} from Eq. (16) is not direct because τ_E is a function of P_{aux}. In order to simplify the computation of P_{aux} we choose $K_E = 1$, i.e. we choose P_{aux} and $P_{rad}(n_I)$ such that

$$\frac{\bar{E}}{\tau_E} = P_\alpha + P_{ohmic} - P_{rad} + P_{aux} = P \tag{17}$$

From the equilibrium equation for the energy E, $0 = -(\bar{E}/\bar{\tau}_E) + \bar{P}$, and the correlation between the energy confinement scaling τ_E and the power P, we realize that the solution for Eq. (17) is $P = \bar{P}$. Therefore, the control strategy will be to adjust P_{aux} and n_I to make P constant and equal to $\bar{P}$ satisfying Eq. (17) and reducing Eq. (12) to

$$\frac{d\tilde{E}}{dt} = -\frac{\tilde{E}}{\tau_E}$$

The subsystem $\tilde{E}$ is exponential stable since $\tau_E > 0$. In practice, there are limitations on the power supply system that constrain the rate at which the auxiliary power can be varied. This condition can be written $|dP_{aux}/dt| < R_{aux}$ where R_{aux} is the maximum auxiliary power ramp rate. It is thought that $R_{aux} \sim 10$–20 MW s^{-1} may be achievable for ITER [3] and this value was used for all the simulations. The controller that implements Eq. (17) is synthesized in two steps:

First Step: We compute P_{aux} as

$$P_{aux} = \bar{P} - [P_\alpha + P_{ohmic} - P_{rad}] \tag{18}$$

If $P_{aux} \geq 0$ then we keep this value for P_{aux} and let $S_I = 0$. If $P_{aux} < 0$ then we take $P_{aux} = 0$ and go to the second step.

Second Step: We look for the least $n_I = n_I^* > 0$ such that

$$-\bar{P} + P_\alpha + P_{ohmic} = P_{rad}(n_I^*) \tag{19}$$

In order to simplify the computation of this solution we need to find an expression for the radiation losses, that can be used for the design of our controller, simpler than the one given by Post et al. in [8] and stated in Eq. (7). Stacey proposes in [13] a simpler law that scales the bremsstrahlung component with $T^{1/2}$, the line component with $T^{-1/2}$ and the recombination component with $T^{-3/2}$. Capturing this physics, we use an approximate law of the form

$$\psi_z^{aprox}(T) = k_b T^{1/2} + k_l T^{-1/2} + k_r T^{-3/2} \tag{20}$$

where the constants k_b, k_l and k_r are adjusted such that $\psi_Z^{aprox}(T) < \psi_Z(T)$ for all T. This law allows the reduction of Eq. (19) to a polynomial equation in n_I, making the search for n_I^* almost trivial. The fact that $\psi_Z^{aprox}(T) < \psi_Z(T)$ guarantees that the approximate n_I^* is always higher than the real n_I^* and there is no risk of losing stability by not injecting enough impurities. As conclusion, no matter how complex the law for the radiation losses may be, there will always be a simple approximation of the radiation loss law that is good enough for control purposes.* and there is no risk of losing stability by not injecting enough impurities. As conclusion, no matter how complex the law for the radiation losses may be, there will always be a simple approximation of the radiation loss law that is good enough for control purposes.

Defining

$$\hat{n}_I = \tilde{n}_I - n_I^*, \quad S_I = \frac{n_I^*}{\tau_I} + S_I^*$$

$$f(\hat{n}_I,\ \tilde{E},\ \tilde{n}_\alpha,\ \tilde{n}_{DT}) = -\left[\frac{\bar{E}}{\tau_E} - (P_\alpha + P_{ohmic} - P_{rad})\right]$$

we can rewrite Eqs. (11) and (12) as

$$\frac{d\hat{n}_I}{dt} = -\frac{\hat{n}_I}{\tau_I} + S_I^*; \quad \frac{d\tilde{E}}{dt} = -\frac{\tilde{E}}{\tau_E} + f(\hat{n}_I,\ \tilde{E},\ \tilde{n}_\alpha,\ \tilde{n}_{DT})$$

We take $V = (\hat{n}_I^2 + \tilde{E}^2)/2$ as our Lyapunov function candidate, write $f = \hat{n}_I\phi$, where ϕ is a continuous function because $f(0, \tilde{E}, \tilde{n}_\alpha, \tilde{n}_{DT}) = 0$, and compute

$$\dot{V} = \hat{n}_I\dot{\hat{n}}_I + \tilde{E}\dot{\tilde{E}} = -\frac{\hat{n}_I^2}{\tau_I} - \frac{\tilde{E}^2}{\tau_E} + \hat{n}_I[S_I^* + \tilde{E}\phi(\hat{n}_I,\ \tilde{E})]$$

We take

$$S_I = \frac{n_I^*}{\tau_I} - \tilde{E}\phi(\hat{n}_I,\ \tilde{E}) - K_I\hat{n}_I, \quad K_I \geq 0 \tag{21}$$

which gives $\dot{V} = -((1/\tau_I) + K_I)\hat{n}_I^2 - (\tilde{E}^2/\tau_E) < 0$ and achieves exponential stability.

We note from Eq. (11) that $\tilde{n}_I$ is input-state stable (ISS) [14] with respect to S_I. This ensures that $\tilde{n}_I$ will be bounded as long as S_I is bounded and exponentially stable once S_I becomes zero.

After stabilizing $\tilde{E}$ using P_{aux} and S_I as controllers, we must focus in Eqs. (8) and (9) to achieve stability for $\tilde{n}_{DT}$ and $\tilde{n}_\alpha$. We apply a backstepping procedure to achieve stability of $\tilde{n}_{DT}$. Toward this goal, we start taking $\tilde{n}_n$ as the virtual control w,

$$\frac{d\tilde{n}_{DT}}{dt} = -\left[\frac{1}{\tau_{DT}} + \bar{n}_{DT}\langle\sigma v\rangle\right]\bar{n}_{DT} - 2\left(\frac{\bar{n}_{DT}}{2}\right)^2\langle\sigma v\rangle + u_{DT} + \frac{w}{\tau_d}$$

since $[(1/\tau_{DT}) + \bar{n}_{DT}\langle\sigma v\rangle]$ is positive, we exponentially stabilize $\tilde{n}_{DT}$ taking w equal to

$$\alpha(n_\alpha,\ n_{DT},\ E) = \tau_d\left[2\left(\frac{\tilde{n}_{DT}}{2}\right)^2\langle\sigma v\rangle - u_{DT}\right] \tag{22}$$

reducing in this way Eq. (9) to

$$\frac{d\tilde{n}_{DT}}{dt} = -\left[\frac{1}{\tau_{DT}} + \bar{n}_{DT}\langle\sigma v\rangle\right]\tilde{n}_{DT}$$

Defining now $z = \tilde{n}_n - \alpha \Leftrightarrow \tilde{n}_n = z + \alpha$, we can write $\dot{z} = \dot{\tilde{n}}_n - \dot{\alpha} = S^* - \dot{\alpha}$. Taking the Lyapunov function candidate $V = (\tilde{n}_{DT}^2/2) + (z^2/2)$, recalling the equations for $\dot{\tilde{n}}_{DT}$ and $\dot{z}$ and taking into account our definition Eq. (22) for α we can compute

$$\dot{V} = \tilde{n}_{DT}\dot{\tilde{n}}_{DT} + z\dot{z}$$

$$\dot{V} = -\left[\frac{1}{\tau_{DT}} + \bar{n}_{DT}\langle\sigma v\rangle\right]\tilde{n}_{DT}^2 + z\left[S^* - \dot{\alpha} + \frac{\tilde{n}_{DT}}{\tau_d}\right]$$

Taking

$$S = -K_S(\tilde{n}_n - \alpha) + \dot{\alpha} - \frac{\tilde{n}_{DT}}{\tau_d} + \frac{n_n}{\tau_d} \tag{23}$$

with $K_s > 0$, we have

$$\dot{V} = -\left[\frac{1}{\tau_{DT}} + \bar{n}_{DT}\langle\sigma v\rangle\right]\tilde{n}_{DT}^2 - K_S z^2 < 0$$

and we achieve exponential stability for $(\tilde{n}_{DT},\ \tilde{n}_n)$.

To have a closed expression for the control law Eq. (23) for S, we compute $\dot{\alpha}$ in terms of $\dot{n}_\alpha$, $\dot{n}_{DT}$, $\dot{n}_I$ and $\dot{E}$ which can be obtained from Eqs. (8)–(12).

We note from Eq. (8) that $\tilde{n}_\alpha$ is ISS (input-state stable) with respect to $\tilde{n}_{DT}$ and u_α. Therefore, since $\tilde{n}_{DT}$ is bounded (because it is exponentially stable), and u_α is bounded (because $\tilde{E}$ is exponentially stable and $\langle\sigma v\rangle$ is a bounded function), $\tilde{n}_\alpha$ will be bounded for all time. In addition, once E converges to $\bar{E}$ ($\tilde{E} \to 0$), n_{DT} converges to $\bar{n}_{DT}$ ($\tilde{n}_{DT} \to 0$) and $n_I = \tilde{n}_I$ converges to $\bar{n}_I = 0$ this equation reduces to

$$\frac{d\tilde{n}_\alpha}{dt} = -\frac{\tilde{n}_\alpha}{\bar{\tau}_\alpha} + u_\alpha^*, \quad u_\alpha^* = -\frac{\bar{n}_\alpha}{\bar{\tau}_\alpha} + \left(\frac{\bar{n}_{DT}}{2}\right)^2\langle\sigma v\rangle$$

The function $\langle\sigma v\rangle$ is a function of $T = (2/3)(\bar{E}/(2\bar{n}_{DT} + 3n_\alpha))$ once $n_I = \tilde{n}_I$ converges to zero, and has a positive derivative in the region of interest. Consequently u_α^* has the same sign as $-\tilde{n}_\alpha/\bar{\tau}_\alpha$ and vanishes when $\tilde{n}_\alpha$ vanishes ($\langle\sigma v\rangle = \langle\bar{\sigma} v\rangle$) because $0 = -(\bar{n}_\alpha/\bar{\tau}_\alpha) + (\bar{n}_{DT}/2)^2\langle\bar{\sigma} v\rangle$ is the equilibrium equation for n_α. This implies exponential stability for $\tilde{n}_\alpha$.

5. Simulation results

It should be noted that our controller can be independent of k_I choosing a sufficiently high value for K_I. Therefore, the choice of $k_I = 10$ can be considered completely arbitrary and with the only purpose of the simulation. In addition, we consider $k_d = 3$, $k_\alpha = 7$.

The controller designed shows capability of rejecting different types of large perturbations in initial conditions. Fig. 1 shows a tested domain of stability for the nonlinear controller. This study is carried out generating initial perturbations around the equilibrium ($\bar{T} = 7.5\ KeV$, $\bar{n}_e = 1.20 \times 10^{20}\ m^{-3}$, $\bar{f}_\alpha = 5.53\%$, $\bar{\beta} = 3\%$, $\bar{n}_\alpha = 6.64 \times 10^{18}\ m^{-3}$, $\bar{n}_{DT} = 1.07 \times 10^{20}\ m^{-3}$, $\bar{E} = 4.21 \times 10^5\ J\ m^{-3}$, $\bar{P}_{aux} = 0\ W\ m^{-3}$, $\bar{S} = 5.52 \times 10^{18}\ m^{-3}\ s^{-1}$) for T and n_e and keeping the alpha-particle fraction $f_\alpha := n_\alpha / n_e$ equal to that of the equilibrium. The figure compares its performance with other two controllers synthesized by linear pole placement [5] and linear robust [6] techniques, for a linearization point very close to our equilibrium point, which use mainly the same dynamical model presented here but considering only the fueling rate as actuator. While the boundaries shown for the linear controllers are absolute, for the nonlinear controller they only indicate the limits within which we performed our tests.

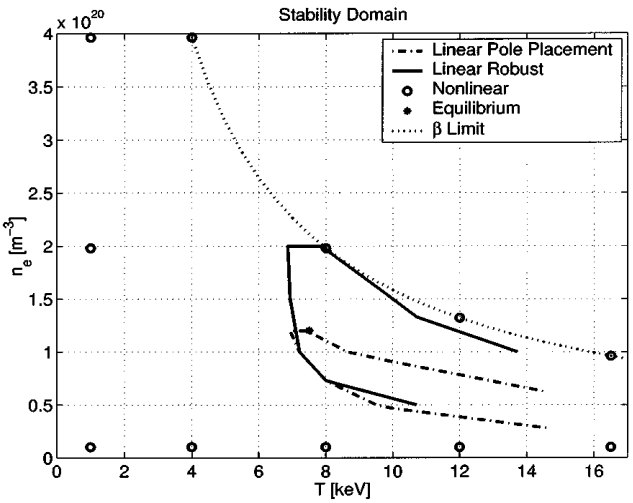

Fig. 1. Stability Domain Comparison.

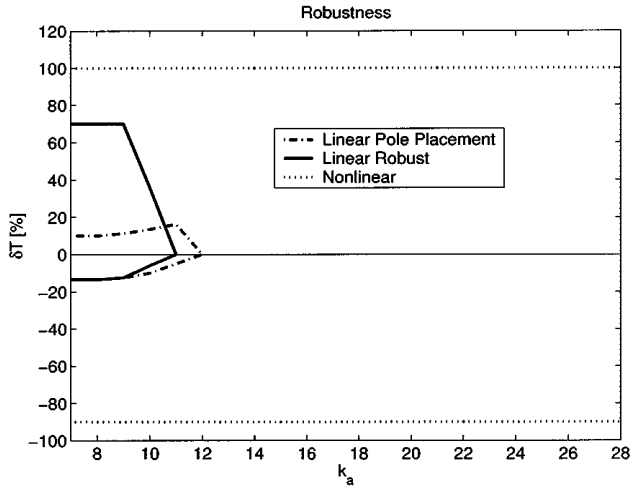

Fig. 2. Robustness against uncertainty in k_α. Comparison with linear controllers synthesized in [5], [6].

The robustness of our controller was also studied against those of the linear controllers. Figs. 2 and 3 show, respectively, the regions of stability against uncertainty in the parameter k_α, whose nominal value is equal to 7, and uncertainty in the parameter k_d, whose nominal value is equal to 1, when the system suffers perturbations in the initial temperature. Again, the region shown for the nonlinear controller is not a limit. With the sole objective to show its performance we tested it against uncertainties up to 400% and perturbations for initial T between -90 and 100%.

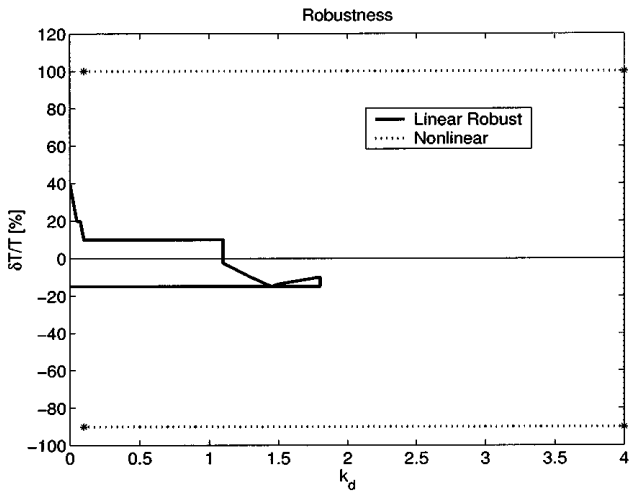

Fig. 3. Robustness against uncertainty in k_d. Comparison with linear controller synthesized in [7] for $k_d = 0$.

6. Conclusions and future work

The information taken into account by the controller when it is synthesized using the full nonlinear model makes it capable of dealing with perturbations in initial conditions that were unmanageable until now. On the other hand, the multi-input nature of the controller allows it to reject large perturbations in initial conditions leading to both thermal excursion and quenching. In addition, the effectiveness of the controller does not depend on whether the operating point is an ignition or a subignition point. Since the nonlinear controller depends parametrically on the equilibrium point, it can drive the system from one equilibrium point to another allowing in this way the change of power, other plasma parameters and ignition conditions. No scheduled controllers are necessary and the same control law is valid for every equilibrium point. The controller can deal with arbitrary values of k_d allowing either pellet injection or gas puffing. Simulation results show good robustness properties against uncertainties in the confinement times.

One possible extension of this work involves developing a one-dimensional (1-D) dynamic model. In this way we would not only achieve results for a plant that is closer to reality but also gain expertise that could be directly applicable to other problems in control of nuclear fusion. Problems like transport control, the improvement of the energy confinement time and MHD stability, among others, require control of not only the values of the density, temperature and current, but also of their profiles.

Acknowledgements

This work was supported by a grant from NSF.

References

[1] S. Mirnov, et al., Chapter 8: Plasma operation and control, Nuclear Fusion, 39 (12) (December 1999) 2251–2389, IAEA.
[2] J. Mandrekas, W.M. Stacey, Jr, Evaluation of different control methods for the thermal stability of the international thermonuclear experimental reactor, Fusion Technology 19 (1) (1991) 57–77.
[3] S.W. Haney, L.J. Perkins, J. Mandrekas, W.M. Stacey, Jr, Active control of burn conditions for the international thermonuclear experimental reactor, Fusion Technology 18 (4) (1990) 606–617.
[4] D. Anderson, T. Elevant, H. Hamen, M. Lisak, H. Persson, Studies of fusion burn control, Fusion Technology 23 (1) (1993) 5–41.
[5] W. Hui, G.H. Miley, Burn control by refueling, Bulletin of the American Physical Society 37 (6) (1992) 1399.
[6] B.A. Bamieh, W. Hui, G.H. Miley, Robust burn control of a fusion reactor by modulation of the refueling rate, Fusion Technology 25 (3) (1994) 318–325.
[7] W. Hui, K. Fischbach, B. Bamieh, G.H. Miley, Effectiveness and constraints of using the refueling system to control fusion reactor burn, in: Proceedings 15th IEEE/NPSS Symposium on Fusion Engineering, vol. 2, 1994, pp. 562–564.
[8] D.E. Post, R.V. Jensen, C.B. Tarter, W.H. Grasberger, W.A. Lokke, Steady-state radiative cooling rates for low-density, high-temperature plasmas, Atomic Data and Nuclear Data Tables 20 (5) (1977) 397–439.
[9] L.M. Hively, Convenient computational forms for Maxwellian reactivities, Nuclear Fusion 17 (4) (1977) 873.
[10] N.A. Uckan, Confinement capability of ITER-EDA design, in: Proceedings of the 15th IEEE/NPSS Symposium on Fusion Engineering, vol. 1, 1994, pp. 183–186.
[11] N.A. Uckan, J. Hogan, W. Houlberg, J. Galambos, L.J. Perkins, S. Haney, D. Post, S. Kaya, ITER design: physics basis for size, confinement capability power levels and burn control, Fusion Technology 26 (3 (part 2)) (1994) 327–330.
[12] Y. Shimomura, et al., ITER-FEAT operation, Nuclear Fusion 41 (3) (2001) 309–316.
[13] W. Stacey, Fusion: An Introduction to the Physics and Technology of Magnetic Confinement Fusion, Wiley, New York, 1984.
[14] H.K. Khalil, Nonlinear Systems, second ed., Prentice Hall, 1996.